PFC/JA-85-18

DETECTION OF ALPHA PARTICLES BY CO_2 LASER SCATTERING

Linda Vahala and George Vahala
Department of Physics - College of William and Mary
Williamsburg, VA 23185

Dieter J. Sigmar
Plasma Fusion Center
Massachusetts Institute of Technology
Cambridge, MA 02139 U. S. A.

JUNE 1985

This work was supported by the U.S. Department of Energy Contract No. DE-AC02-78ET51013. Reproduction, translation, publication, use and disposal, in whole or in part by or for the United States government is permitted.

DETECTION OF ALPHA PARTICLES BY CO_2 LASER SCATTERING

Linda Vahala and George Vahala

Department of Physics

College of William & Mary

Williamsburg, VA 23185

and

D. J. Sigmar

Plasma Fusion Center

Massachusetts Institute of Technology

Cambridge, MA 02139

U. S. A.

ABSTRACT

It is shown that the alpha particle contribution to the scattered power can be dominant in the coherent scattering of CO_2 laser in a Maxwellian plasma. The optimal forward scattering angle is around 1.0° with detection of the electron density fluctuation wavenumbers $k_\perp >> k_\parallel$ (relative to the toroidal magnetic field). Because of the strong dependence of the scattered signal on the alpha particle temperature and the alpha distribution function, it seems feasible that CO_2 laser scattering, with clever heterodyne techniques, could give detailed local information on fusion alphas.

1. INTRODUCTION

Recently, there has been considerable experimental interest [1-5] in the use of CO_2 laser scattering to investigate certain collective effects in plasmas. In the scattering of electromagnetic waves from a charged particle, the radiated power is proportional to (particle mass)$^{-2}$. Thus, the scattering is principally from the electrons. If collective or ion information is required then one must resort to long wavelength lasers so as to probe the plasma around the electrons. Also, since one wishes to use the laser as a passive diagnostic tool, the incident laser frequency should be chosen much higher than the electron plasma frequency ω_{pe} or the electron gyrofrequency Ω_e. As a result the plasma is optically thin, with nearly all the incident power passing straight through the plasma. A ruby laser with (short) wavelength 6.9×10^{-5} cm is standardly used to study single-particle aspects of electron behavior in fusion plasmas. The longer wavelength CO_2 laser (wavelength 1.06×10^{-3} cm) can be used to study collective aspects of electron behavior, but very small forward scattering angles are required. Unfortunately, lasers with longer wavelength than the CO_2 laser are not presently available at the required high incident power densities.

In this paper we investigate the possibility of using CO_2 laser scattering to detect alpha particles by calculating the scattering function $S(\overrightarrow{k},\omega)$ of a magnetized plasma, as a function of various models for the alpha particle velocity distribution.

Since the theoretical formulation of electromagnetic scattering in plasma has been presented in detail in, for example, Sheffield [6] and in Slusher and Surko [1] we shall be very brief about the fundamentals and concentrate on the application. A preliminary report not allowing for the important effects of the magnetic field was written by Hutchinson, et al. [7].

2. COHERENT SCATTERING FROM ELECTRON DENSITY FLUCTUATIONS

The scattering geometry is shown schematically in Fig.1. The background plasma is assumed Maxwellian for both electrons and ions, with temperatures $T_i = T_e = 10$ keV and densities $n_{eo} = 1.2 \times 10^{14}$ cm^{-3} and $n_{io} = 1.196 \times 10^{14}$ cm^{-3}. Because the plasma scattering volume V is rather localized in the plasma, we assume a uniform toroidal magnetic field with $B_0 = 50$ kG. Several alpha particle distribution functions are considered using various effective "temperatures" T_α with density $n_{\alpha o} = 7.5 \times 10^{11}$cm^{-3}. Thus for the CO_2 laser, with incident frequency $\omega_I = 2.8 \times 10^{14}$ Hz, we have

$$\omega_I >> \omega_{pe} > \Omega_e >> \omega_{pi} > \omega_{p\alpha} > \Omega_i > \Omega_\alpha \tag{1}$$

For alpha particle temperatures of interest here ($T_\alpha > 50$ keV), we find that the alpha particle Larmor radius $\rho_\alpha >> L \sim V^{1/3}$, the plasma scattering length. Thus we can treat the alphas as unmagnetized. The electrons and ions are treated as magnetized. The electrons are assumed to be nonrelativistic (though this assumption becomes less justified for $T_e > 10$ keV). Because of the high incident laser frequency, Eq.(1), there is negligible attenuation of the incident laser beam so that all electrons in the scattering volume V interact with the same incident laser electric field $\vec{E}_I$. Moreover, the incident laser power is such that

$$\frac{P_I}{A} << \frac{m_e^2 v_e^2}{8\pi e^2} \omega_I^2$$

(A is the cross section area of the laser beam, v_e is the electron thermal speed) so that the plasma is not perturbed by the incident laser. This permits us to treat the equilibrium background plasma in the linear approximation, using the Rostocker superposition principle for dressed test particles.

It is readily shown [1, 6] that the power scattered into the solid angle $d\Omega$ is

$$P_s \, d\Omega \, \frac{d\omega}{2\pi} = P_I \, r_0^2 \, n_{eo} \, L \, d\Omega \, \frac{d\omega}{2\pi} \, S(\vec{k}, \omega) \tag{2}$$

where P_I is the incident laser power, and $r_0^2 = 8 \times 10^{-26}$ cm^2 is the Thomson cross section. It is to overcome this very small Thomson scattering cross section that one must resort to high power lasers. $S(\vec{k}, \omega)$ is the electron spectral density correlation function or scattering function

$$S(\vec{k}, \omega) \simeq \frac{|n_{e1}(\vec{k}, \omega)|^2}{n_{eo}} \tag{3}$$

with perturbed electron density n_{e1}, and < > represents an ensemble average over initial particle phase space coordinates. $\vec{k} = \vec{k}_S - \vec{k}_I$ and $\omega = \omega_S - \omega_I$ are the wave vector and frequency shift due to the incident wave-plasma interaction. For the scattering under consideration here $|\vec{k}_S| \simeq |\vec{k}_I|$ so that $|\vec{k}| = 2 \, k_I \sin \theta/2$ (see Fig.1).

Following standard procedures [1, 6] for a thermal magnetized plasma with unmagnetized alphas under the longitudinal approximation, one readily finds that the electron spectral density correlation function can be separated into 3 parts

$$S\,(\overrightarrow{k,\omega}) = S_e\,(\overrightarrow{k,\omega}) + S_i\,(\overrightarrow{k,\omega}) + S_\alpha\,(\overrightarrow{k,\omega}) \qquad (4)$$

where, for Maxwellian distributions,

$$S_e\,(\overrightarrow{k,\omega}) = \frac{|1 + H_i + G_\alpha|^2}{|\varepsilon_L|^2}\;\frac{2\pi^{1/2}}{|k_\parallel| v_e}\sum_{\ell=-\infty}^{\infty} e^{-k_\perp^2\rho_e^2}\, I_\ell\,(k_\perp^2\rho_e^2)\,\exp\left(-\frac{(\omega - \ell\Omega_e)^2}{k_\parallel^2 v_e^2}\right) \qquad (5)$$

$$S_i\,(\overrightarrow{k,\omega}) = \frac{|H_e|^2}{|\varepsilon_L|^2}\;\frac{n_{io}}{n_{eo}}\;\frac{2\pi^{1/2}}{|k_\parallel| v_i}\sum_{\ell=-\infty}^{\infty} e^{-k_\perp^2\rho_i^2}\, I_\ell\,(k_\perp^2\rho_i^2)\,\exp\left(-\frac{(\omega - \ell\Omega_i)^2}{k_\parallel^2 v_i^2}\right) \qquad (6)$$

and

$$S_\alpha\,(\overrightarrow{k,\omega}) = \frac{|\alpha^2\,[1 + \zeta_e\, Z(\zeta_e)]|^2}{|\varepsilon_L|^2}\;\frac{4n_{\alpha o}}{n_{eo}}\;\frac{2\pi^{1/2}}{|\vec{k}| v_\alpha}\quad\exp\left(-\frac{\omega^2}{|\vec{k}|^2 v_\alpha^2}\right) \qquad (7)$$

The dielectric function is

$$\varepsilon_L = 1 + H_e(\overrightarrow{k,\omega}) + H_i(\overrightarrow{k,\omega}) + G_\alpha(\overrightarrow{k,\omega}) \qquad (8)$$

with

$$H_e = \alpha^2 \sum_\ell e^{-k_\perp^2\rho_e^2}\; I_\ell\,(k_\perp^2\rho_e^2)\left[1 + \frac{\omega}{k_\parallel v_e}\; Z\left(\frac{\omega - \ell\Omega_e}{k_\parallel v_e}\right)\right] \qquad (9)$$

$$H_i = \alpha^2\,\frac{n_{io}}{n_{eo}}\,\frac{T_e}{T_i}\sum_\ell e^{-k_\perp^2\rho_i^2}\; I_\ell\,(k_\perp^2\rho_i^2)\left[1 + \frac{\omega}{k_\parallel v_i}\, Z\left(\frac{\omega - \ell\Omega_i}{k_\parallel v_i}\right)\right], \qquad (10)$$

and for the unmagnetized Maxwellian alphas

$$G_\alpha = \alpha^2\,\frac{4n_{\alpha o}}{n_{eo}}\;\frac{T_e}{T_\alpha}\;\left[1 + \zeta_\alpha\; Z(\zeta_\alpha)\right] \qquad (11)$$

The gyroradii

$$\rho_e^2 = v_e^2/2\Omega_e^2 \ , \ \rho_i^2 = v_i^2/2\Omega_i^2$$

and

$$\zeta_\alpha = \alpha \frac{\omega}{\omega_{p\alpha}} \left(\frac{2n_{\alpha o}}{n_{eo}} \frac{T_e}{T_\alpha} \right)^{1/2} ,$$

$$\zeta_\alpha = \alpha \frac{\omega}{2^{1/2}\omega_{pe}}$$

with the plasma dispersion function for Im $\zeta > 0$

$$Z(\zeta) = \frac{1}{\pi^{1/2}} \int_{-\infty}^{\infty} dx \frac{e^{-x^2}}{x - \zeta}$$

and analytic continuation for Im $\zeta < 0$.

The so-called Salpeter parameter

$$\alpha = (|\vec{k}| \lambda_{De})^{-1} \tag{12}$$

where the electron Debye length $\lambda_{De} = v_e/2^{1/2}\omega_{pe}$.

Since the dielectric function $\varepsilon_L \to 1$ as $\alpha \to 0$, the Salpeter parameter is an indication of the strength of collective processes within the plasma. $S_e(\vec{k},\omega)$ is due to both free electrons moving in their unperturbed gyro-orbits as well as from electrons shielding these test particles electrons. $S_i(\vec{k},\omega)$ and $S_\alpha(\vec{k},\omega)$ are contributions from the scattering off electrons shielding the ions and alphas, respectively. For collective effects to be important we require $\alpha \sim 1$ and only under these conditions can one observe any alpha particle effects on the scattered radiated power. Since, for CO_2 laser scattering and $T_e = 10$ keV,

$$\alpha = \frac{0.0124}{\sin\ \theta/2} \tag{13}$$

we will require very small forward angle scattering: $\theta < 1.4°$. However, using heterodyne techniques and accurate optics the experimentalist can detect down to scattering angles [3] of $\theta = 0.5°$.

3. ALPHA PARTICLE CONTRIBUTION TO SCATTERED RADIATION

To investigate the importance of alpha particles on the total scattered power we plot $S_\alpha(\vec{k},\omega)$,Eq.(7), and the total scattering density $S(\vec{k},\omega)$ for various forward scattering angles θ and angles ϕ with $k_\parallel = k \cos\phi$, $k_\perp = k \sin\phi$. The experimental frequency range of interest is 5 GHz $< w <$ 25 GHz. It is typically found that for $\omega < 3 - 5$ GHz, the ion contribution $S_i(\vec{k},\omega)$ dominates the total scattering density $S(\vec{k},\omega)$; but for higher frequencies S_i becomes negligible.

In Fig.2, $S(\vec{k},\omega)$ and $S_\alpha(\vec{k},\omega)$ are shown as a function of ω for $\theta = 0.5°$, $\phi = 45°$. For this very small forward scattering the Salpeter parameter $\alpha = 2.85$. Nevertheless, for $k_\parallel = k_\perp$, we find that the alpha particle contribution to the scattered power is negligible: $S_\alpha << S$. For $\omega > 4$ GHz, the electrons (free and screening) dominate the scattering density $S_e \simeq S$ with a slow decay of the spectral density with frequency ω. Decreasing the alpha particle temperature from $T_\alpha = 300$ keV to 200 keV has little effect on the total spectral density $S(\vec{k},\omega)$.

On increasing ϕ to $\phi = 85°$ so that $k_\parallel << k_\perp$ but still keeping the collective parameter $\alpha = 2.85$ (i.e., $\theta = 0.5°$), it is still seen that $S_\alpha << S$ — Fig.3. However, the spectral density S rapidly decreases with frequency. For $\omega > 6$ GHz, S_α is very little affected by the increase in ϕ.

However, for scattering angle θ =1.0° (with α = 1.42) and $k_\parallel << k_\perp$, we find a very high resonance peak at ω = 21 GHz, Fig.4. Moreover, for ω > 6 GHz the alpha contribution totally dominates the spectral density function $S_\alpha(\vec{k},\omega) = S(\vec{k},\omega)$ with a plateau in S for 7 GHz < ω < 17 GHz at T_α = 500 keV. On decreasing the alpha particle temperature to 300 keV we still find $S_\alpha \simeq S$ for ω > 6 GHz, but now the resonance amplitude has decreased by nearly two orders of magnitude. This resonance can be identified with the lower hybrid resonance, whose dispersion relation for a cold plasma is given by

$$\omega^2 = \left(1 + \frac{m_i}{m_e}\,\frac{k_\parallel^2}{k_\perp^2}\right) \frac{\omega_{pi}^2}{1 + \omega_{pe}^2/\Omega_e^2} \tag{14}$$

There is also a significant decrease in S for ω > 13 GHz due to decreasing T_α. This is further illustrated in Fig.5. Note that at T_α = 100 keV, $S_\alpha << S$ for ω > 10 GHz. Moreover, increasing $k_\parallel/k_\perp$ with θ = 1.0° and T_α = 200 keV leads to a slightly reduced spectral density S with $S_\alpha \simeq S$, Fig.6. As can be seen from Eq.(14) the lower hybrid resonance frequency also increases with increasing $k_\parallel/k_\perp$ and this accounts for the absence of any resonance structure in S for ω < 17GHz.

In Figs 7-9 we consider the effect of decreasing the Salpeter parameter α = 2.85 (θ = 0.5°) to α = 0.95 (θ = 1.5°) for ϕ = 60° ($k_\perp = 1.73\, k_\parallel$) at T_α = 200 keV. As the forward scattering angle θ increases, the plateau height in the spectal density S — which typically occurs for frequencies ω > 9 GHz — first decreases till θ = 1.1° and then increases by an order of magnitude by θ = 1.5°. In most cases $S_\alpha << S$ and only for a small frequency range is the alpha contribution to the total spectral density significant (see Fig.9 for θ = 1.1° in the frequency range 7 GHz $< \omega <$ 10 GHz).

For $\theta = 1.0°$ but $k_\parallel << k_\perp$ with $\phi = 89°$, we find a very strong lower hybrid wave resonance at $\omega = 7$ GHz, with the total spectral density S being totally dominated by the alpha contribution S_α in the complete frequency range of interest. The effect of alpha particle temperature is to increase the detectable frequency signal range from $\omega_{max} = 9$ GHz for $T_\alpha = 50$ keV to $\omega_{max} = 20$ GHz for $T_\alpha = 300$ keV (Fig.10). If one decreases ϕ to $\phi = 75°$, so that $k_\parallel/k_\perp$ increases by a factor of about 20 from its value at $\phi = 89°$, the lower hybrid resonance is pushed into an undetectable frequency range with $S_\alpha < S$ for all frequencies, Fig.11. With the electron contribution giving a major contribution to the total spectral density S we start to see the beginnings of a plateau in S. If one now decreases the scattering angle to $\theta = 0.5°$ at $T_\alpha = 50$ keV we find a much reduced signal even at $\phi = 89°$ (but still the alpha contribution dominates the spectral density), Fig.12. However, at $\phi = 75°$ the alpha contribution S_α is now negligible. Note again the plateau that forms in S — this being due to the electron contribution.

It is also of interest to consider an alpha particle distribution function of the form

$$f_{\alpha o}(v) \sim v^2 \exp(-v^2/v_\alpha^2) \qquad (15)$$

modelling a loss effect for lower energies. For $T_\alpha = 300$ keV, $\phi = 85°$ ($k_\parallel << k_\perp$) we again find that for $\theta = 1.0°$ the alpha contribution dominates the spectral density function, with the lower hybrid resonance level now being approximately ten times higher than that for the Maxwellian alpha distribution (see also Fig.3). Increasing or decreasing the scattering angle from $\theta = 1.0°$ leads to a reduced alpha contribution to S, Fig.13.

4. SUMMARY AND CONCLUSION

For a Maxwellian plasma with $T_i = T_e = 10$ keV, we find that as the forward scattering angle θ increases from $\theta = 0.5°$ to $1.1°$ the Salpeter parameter α decreases as well as the electron contribution S_e to the total spectral density S. On the other hand the alpha contribution S_α increases. As θ further increases from $\theta = 1.1°$ to $1.5°$ the electron contribution to S now increases and becomes more important than the slowly increasing alpha particle contribution.

The background ion contribution to S is negligible for frequencies $\omega > 5$ GHz.

The optimal observing angle ϕ is that which is nearly perpendicular to the toroidal magnetic field ($\phi > 85°$). Under these circumstances the alpha particle contribution to S $(\vec{k},\omega)$ totally dominates the electron contribution.

A resonance peak, corresponding to the lower hybrid resonance, is also seen for $k_\parallel << k_\perp$.

The use of a loss-cone type distribution for the alpha particles, Eq.(15), rather than a Maxwellian leads to an enhanced alpha contribution to S $(\vec{k},\omega)$. This sensitivity to the shape of f_α is precisely the purpose of this diagnostic.

In conclusion, it appears that with suitable choice of local oscillators with which to perform the heterodyne detection in the frequency range 5 GHz $< \omega <$ 25 GHz one should be able to detect alpha particle contributions to the scattered power and thereby infer the shape of alpha distribution function. For a 100 MW CO_2 laser

$$P_s \, d\Omega d\omega = 3 \times 10^{-3} \, S \, \overrightarrow{(k,\omega)} \, d\Omega d\omega$$

We further suggest that by appropriate focusing of these linear oscillators, one should be able to localize the scattering plasma volume V under consideration and due to the easy access to the tokamak for near forward scattering one may be able to probe different vertical chords through the plasma cross section rather than just the "diameter" chord illustrated in Fig.1.

ACKNOWLEDGEMENTS

This work was performed under contract with U. S. Department of Energy at William and Mary, Oak Ridge National Laboratory and Massachusetts Institute of Technology. We thank J. Sheffield for stimulating discussions.

REFERENCES

[1] SLUSHER, R. E., SURKO, C. M., Phys. Fluids, 23 (1980) 472.

[2] SURKO, C. M., SLUSHER, R. E., Phys. Fluids, 23 (1980) 2425.

[3] SLUSHER, R. E., et al., Phys. Fluids, 25 (1982) 457.

[4] KASPAREK, W., HOLZHAUER, E., Phys. Rev., A27 (1983) 1737.

[5] VALLEY, J. F., SLUSHER, R. E., Rev. Sci. Instrum., 54 (1983) 1157.

[6] SHEFFIELD, J. "Plasma Scattering of Electromagnetic Radiation" Academic Press, New York, 1975.

[7] HUTCHINSON, D. P., VANDERSLUIS, K. L., SHEFFIELD, J., SIGMAR, D. J., "Feasibility of Alpha Particle Measurement by CO_2 Laser Thomson Scattering", ORNL-TM9090 (1985).

FIGURE CAPTIONS

Figure 1 Schematic diagram of the laser scattering geometry. Incident beam of wavenumber k_I, and scattered wavelength k_S. θ is the forward scattering angle. $k = k_S - k_I$, and ϕ is the angle between k and the toroidal magnetic field B_o. $k = 2k_I \sin \theta/2$.

Figure 2 Plot of the spectral density function S (k,ω) vs. $\omega = \omega_S - \omega_I$ for frequency range 1 GHz $< \omega <$ 27 GHz for $\theta = 0.5°$ (Salpeter parameter $\alpha = 2.85$) and $\phi = 45°$ $(k_\parallel = k_\perp)$. S^I_{tot} is the total spectral density for T_α = 200 keV with S^I_α being the alpha particle contribution to S^I_{tot}. S^{II} is for T_α = 300 keV. It should be noted that $S = 10^{-12}$ will yield a scattered power density $P_s = 3 \times 10^{-15}$ watts for a 100 MW laser (see Eq. 16). Experimentally (see Ref. 3) power levels of 5×10^{-13} watts have been readily detected in CO_2 laser scattering.

Figure 3 S (k,ω) vs. ω for $\theta = 0.5°$ but $\phi = 85°$ $(k_\perp >> k_\parallel)$.

Figure 4 S (k,ω) vs. ω for $\theta = 1.0°$ $(\alpha = 1.43)$ and $\phi = 85°$ for I: T_α = 300 keV and II: T_α = 500 keV. Notice that $S_\alpha \simeq S_{tot}$, and the appearance of a resonance at the lower hybrid frequency.

Figure 5 The effect of decreasing T_α on S (k,ω) for $\theta = 1.0°$, $\phi = 85°$.

Figure 6 Effect of $k_\perp/k_\parallel$ on S (k,ω) for $\theta = 1.0°$ and T_α = 200 keV.

Figure 7 The effect of decreasing the collective Salpeter parameter α by increasing $\theta = 0.5°$ (curves I) to $\theta = 0.7°$ (curves II) on S (k,ω). Notice that S_{tot} decreases but the alpha particle contribution S_α is enhanced. $\phi = 60°$ and T_α = 200 keV.

Figure 8 The trend of Fig. 7 continues as α decreases due to increasing forward scattering angle $\theta = 0.7°$ (curves I), $\theta = 0.8°$ (curves II), $\theta = 0.9°$ (curves III).

Figure 9 Further increase of $\theta = 1.1°$ to $\theta = 1.5°$ at $\phi = 60°$ and $T_\alpha = 200$ keV.

Figure 10 The effect of decreasing T_α on $S(k,\omega)$ for $k_\perp >> k_\parallel$ ($\phi = 89°$) and forward scattering angle $\theta = 1.0°$. Notice the high lower hybrid resonance peak in $S(k,\omega)$. For these optimal angles $S_\alpha \approx S_{tot}$.

Figure 11 The effect of decreasing $k_\perp/k_\parallel$ ratio on $S(k,\omega)$ for $\theta = 1.0°$ and low $T_\alpha = 50$ keV. For $\phi = 89°$, $S_\alpha^I \approx S_{tot}^I$, but at $\phi = 75°$ the alpha particle contribution is significantly reduced, $S_\alpha^{II} < S_{tot}^{II}$.

Figure 12 The effect of decreased scattering angle $\theta = 0.5°$ on $S(k,\omega)$ with $T_\alpha = 50$ keV. For $\phi = 89°$ we still find that the alpha particle contribution dominates $S(k,\omega)$ but the signal amplitude is very much reduced over that for $\theta = 1.0°$ (see Fig. 11). For $\phi = 75°$, the alpha particle contribution is negligible, $S_\alpha^{II} << S_{tot}^{II}$.

Figure 13 The scattering density $S(k,\omega)$ for a loss-cone type alpha particle distribution function, Eq. 15. $T_\alpha = 300$ keV and $\phi = 85°$. As the collective parameter increases: $\theta = 1.2°$ ($S_\alpha^I < S_{tot}^I$), $\theta = 1.0°$ ($S_\alpha^{II} \approx S_{tot}^{II}$), $\theta = 0.8°$ ($S_\alpha^{III} < S_{tot}^{III}$). Note that the spectral density amplitude is increased over that for a Maxwellian alpha distribution function.

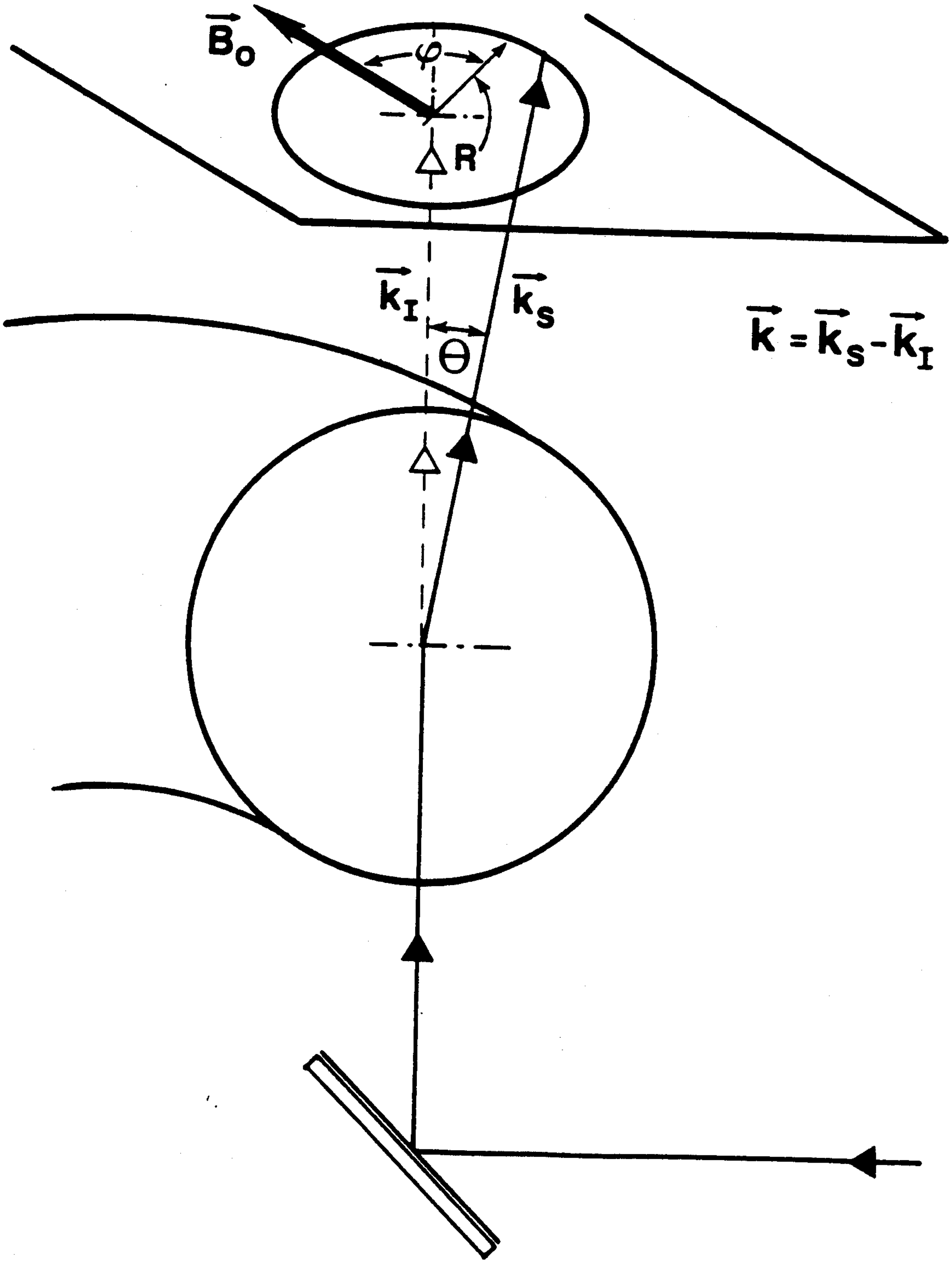

Figure 1

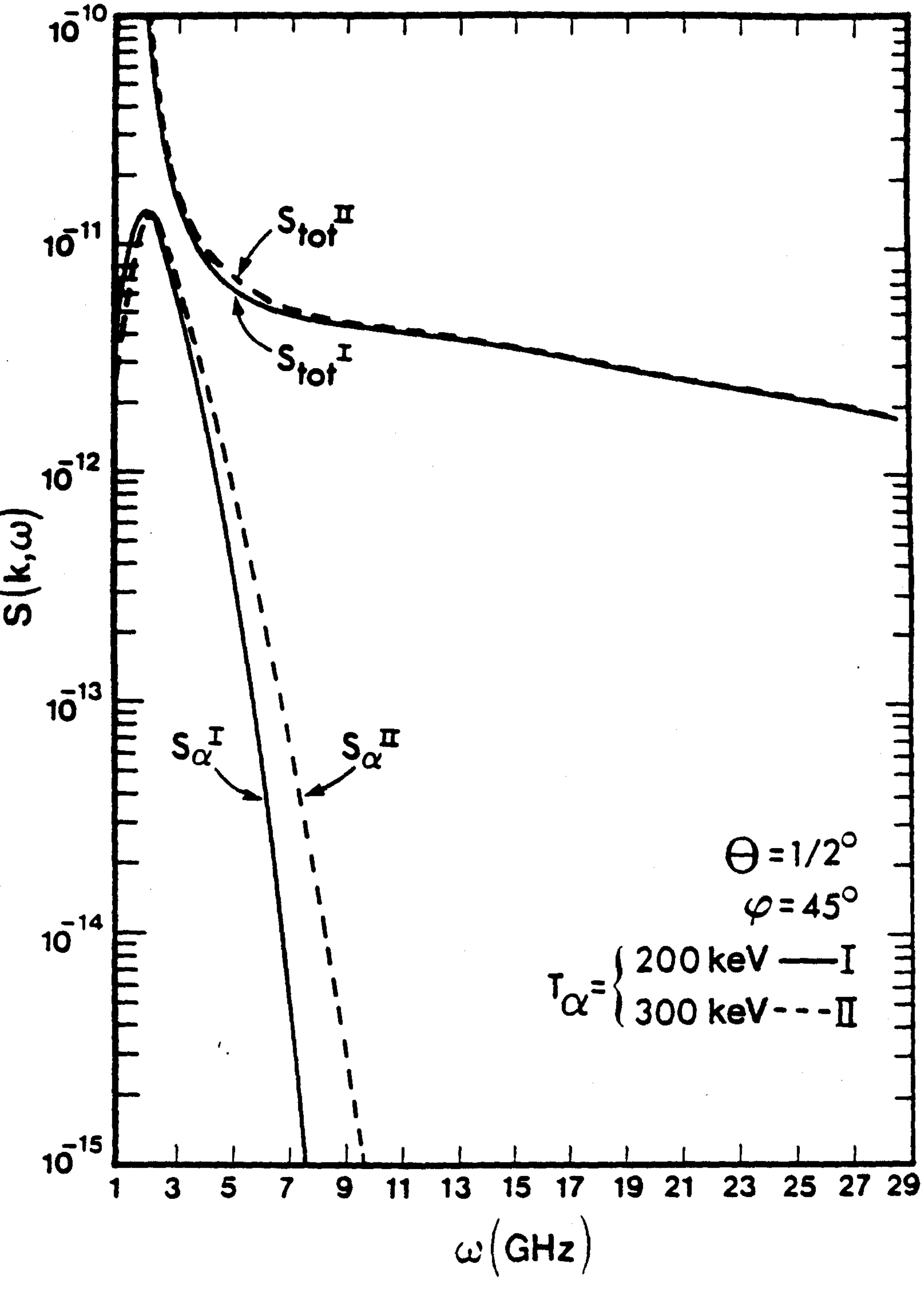

10^{-10}
10^{-11}
10^{-12}
10^{-13}
10^{-14}
10^{-15}
$S(k,\omega)$
S_{tot}^{II}
S_{tot}^{I}
S_{α}^{I}
S_{α}^{II}
$\Theta = 1/2°$
$\varphi = 45°$
$T_{\alpha} = \{$ 200 keV — I
300 keV - - - II
1 3 5 7 9 11 13 15 17 19 21 23 25 27 29
ω (GHz)

Figure 2

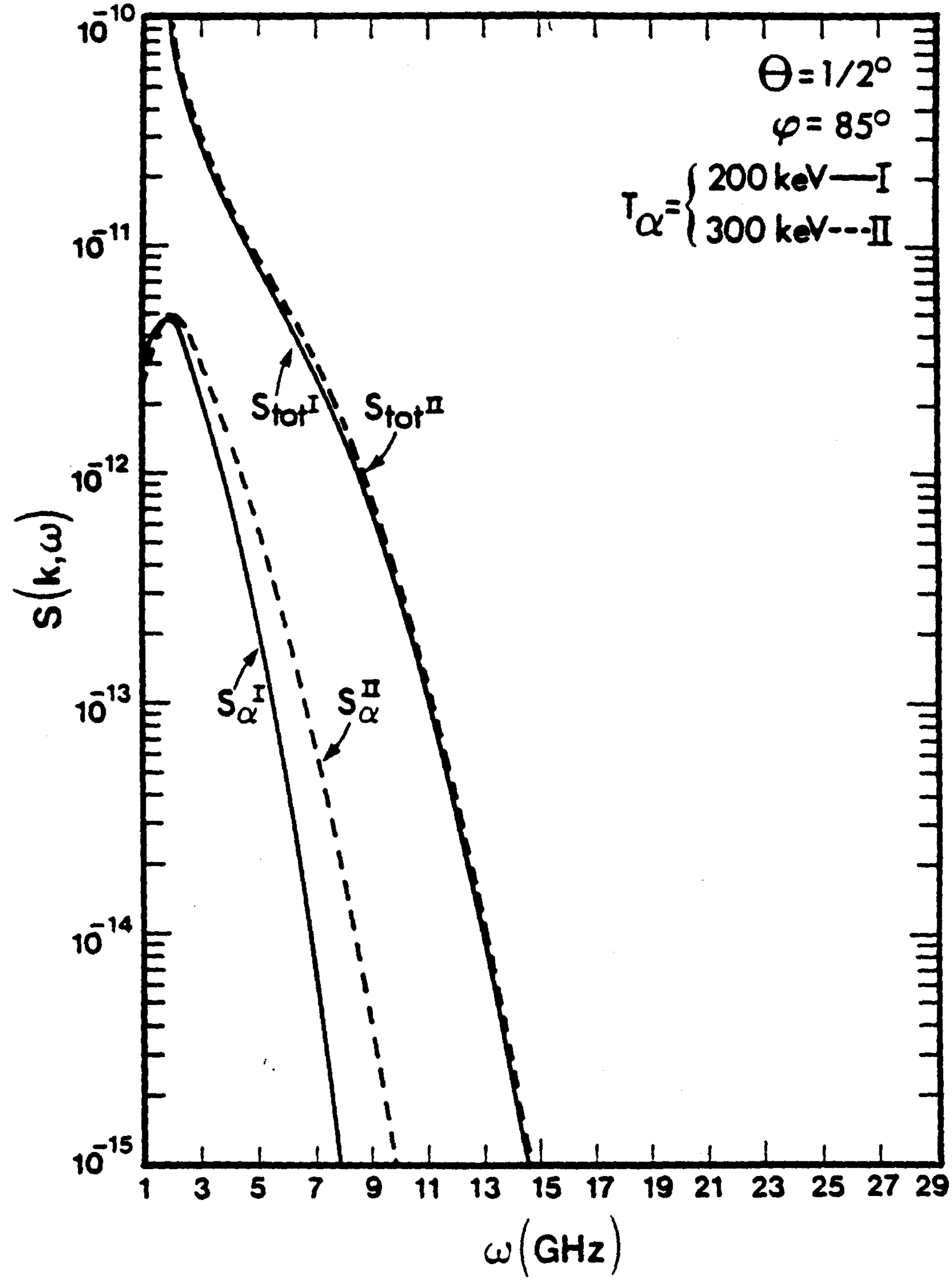

Θ = 1/2°
φ = 85°
T_α = { 200 keV — I ; 300 keV --- II }
S_{tot}^{I}
S_{tot}^{II}
S_α^{I}
S_α^{II}
S(k,ω)
ω (GHz)
10^{-10}
10^{-11}
10^{-12}
10^{-13}
10^{-14}
10^{-15}
1 3 5 7 9 11 13 15 17 19 21 23 25 27 29

Figure 3

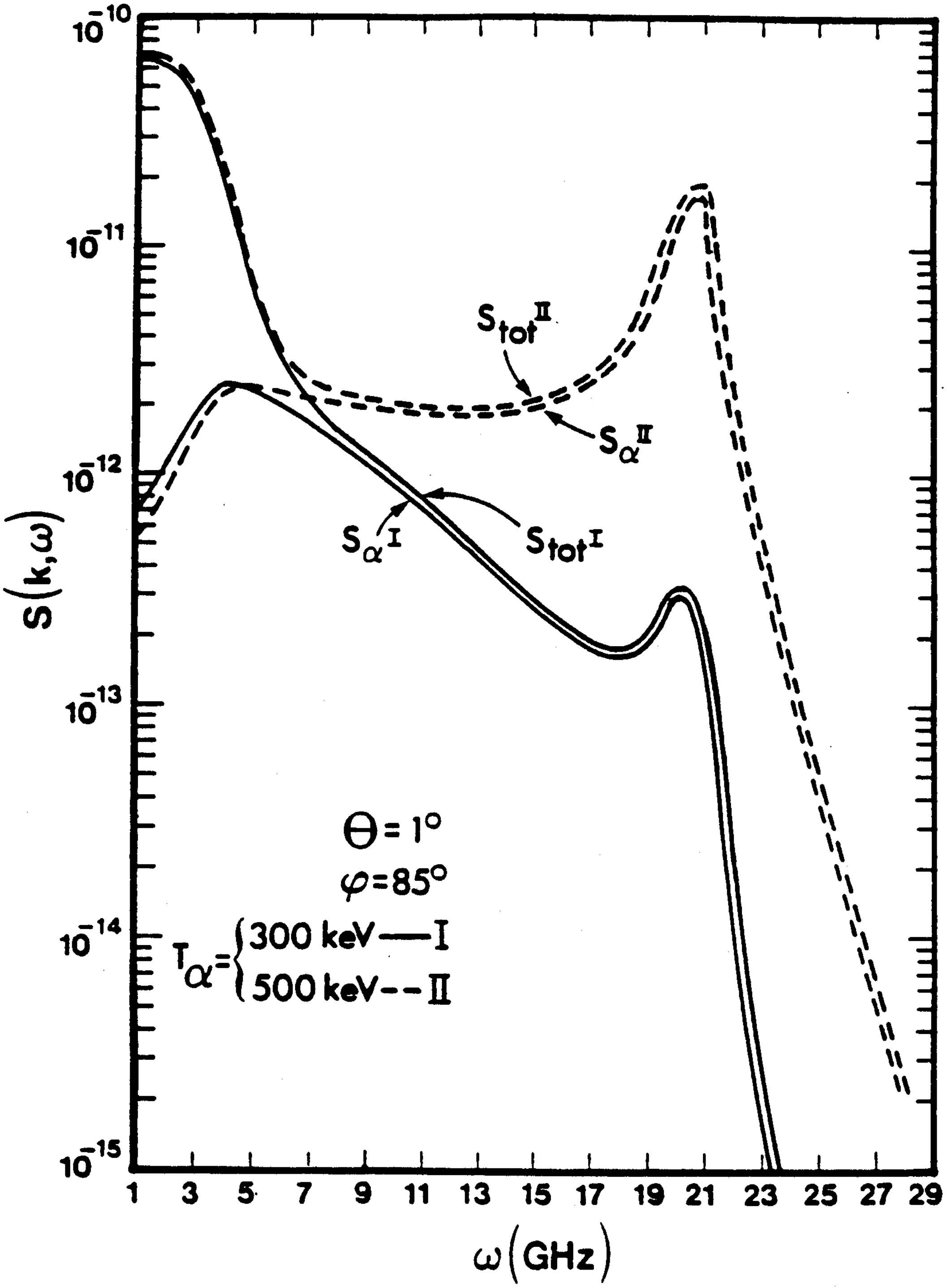

10^{-10}
10^{-11}
10^{-12}
10^{-13}
10^{-14}
10^{-15}
1 3 5 7 9 11 13 15 17 19 21 23 25 27 29
ω(GHz)
S(k,ω)
S_{tot}^{II}
S_{α}^{II}
S_{α}^{I}
S_{tot}^{I}
Θ = 1°
φ = 85°
T_{α} = { 300 keV — I
500 keV -- II

Figure 4

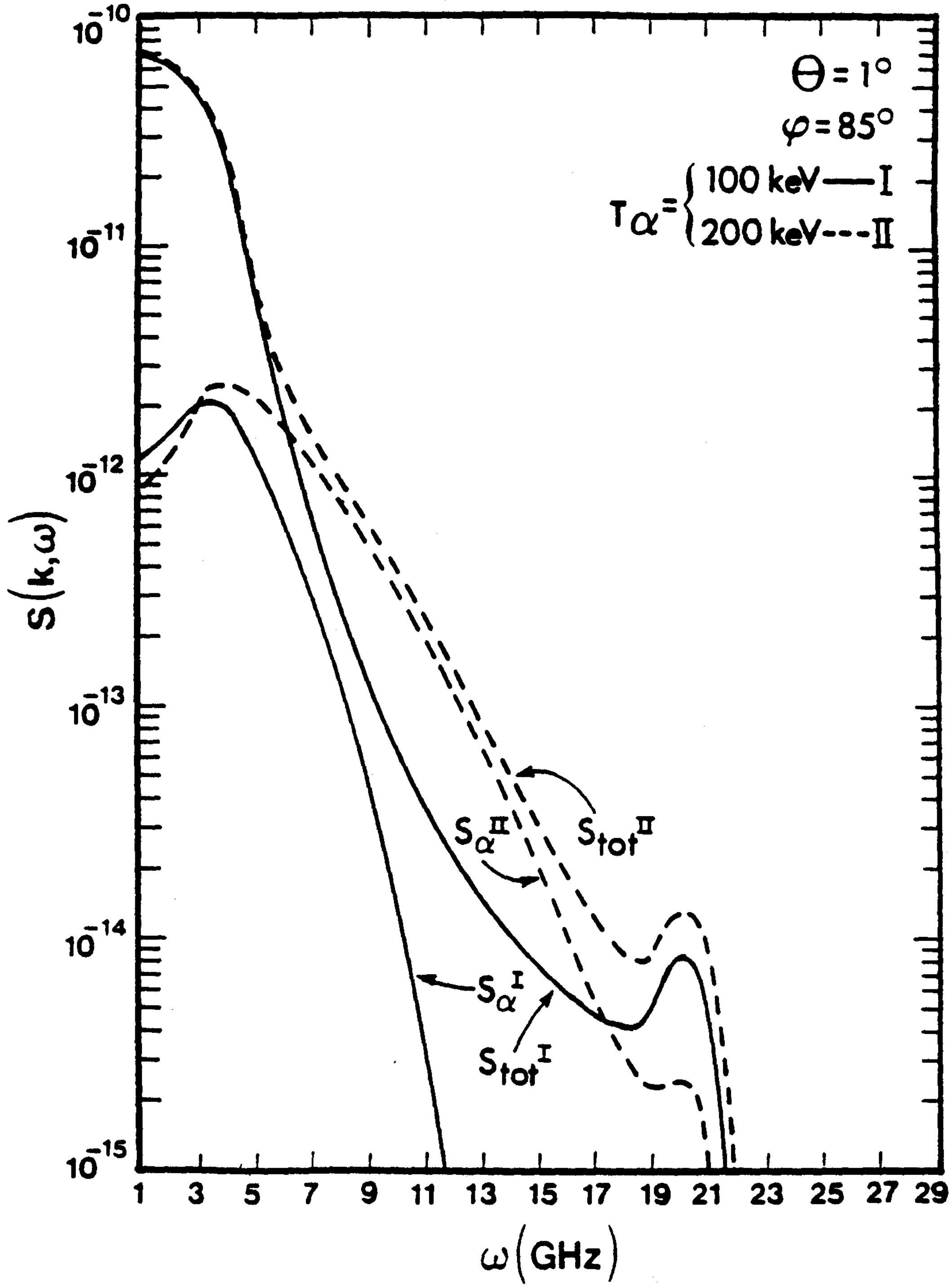

10^{-10}
10^{-11}
10^{-12}
10^{-13}
10^{-14}
10^{-15}
$S(k,\omega)$
$\Theta = 1°$
$\varphi = 85°$
$T_\alpha = \begin{cases} 100\ keV — I \\ 200\ keV --- II \end{cases}$
S_{tot}^{II}
S_α^{II}
S_α^{I}
S_{tot}^{I}
1 3 5 7 9 11 13 15 17 19 21 23 25 27 29
ω (GHz)

Figure 5

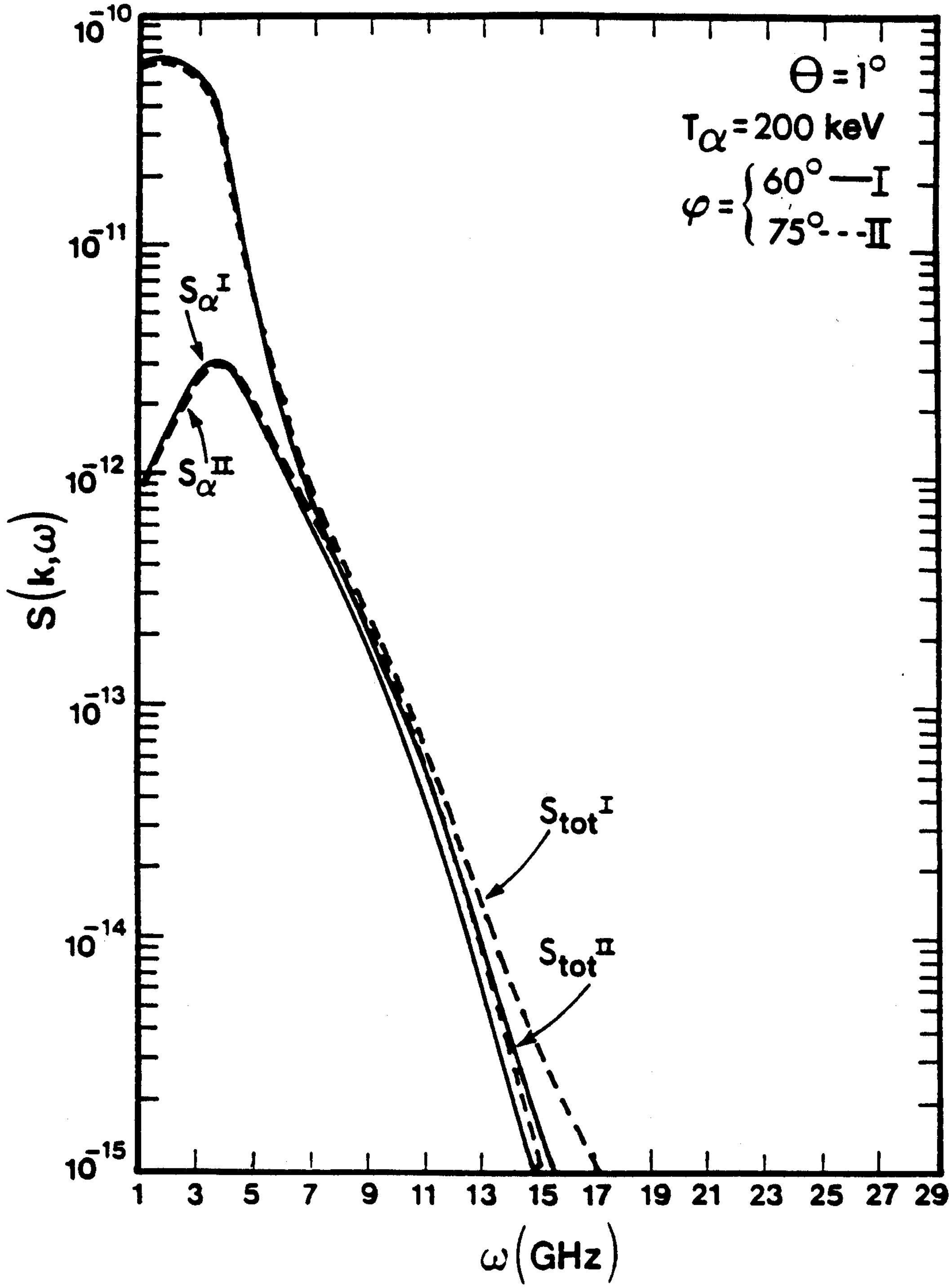

Θ = 1°
T_α = 200 keV
φ = { 60° — I
75° - - II
S_α^{I}
S_α^{II}
S_{tot}^{I}
S_{tot}^{II}
S(k,ω)
ω(GHz)
10^{-10}
10^{-11}
10^{-12}
10^{-13}
10^{-14}
10^{-15}
1 3 5 7 9 11 13 15 17 19 21 23 25 27 29

Figure 6

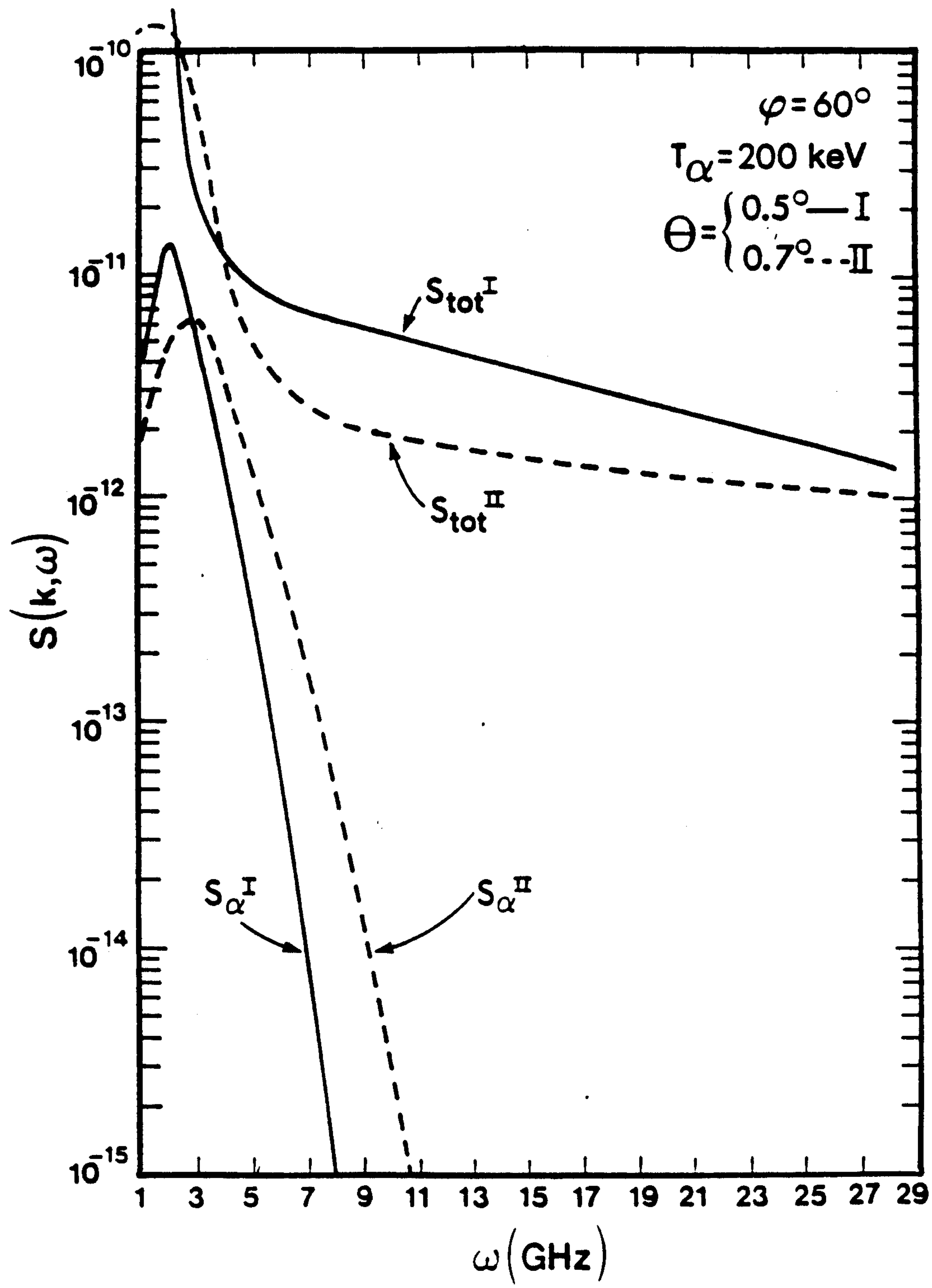

$\varphi = 60°$
$T_\alpha = 200$ keV
$\Theta = \begin{cases} 0.5° — I \\ 0.7° - - II \end{cases}$
S_{tot}^{I}
S_{tot}^{II}
S_α^{I}
S_α^{II}
$S(k,\omega)$
10^{-10}
10^{-11}
10^{-12}
10^{-13}
10^{-14}
10^{-15}
1 3 5 7 9 11 13 15 17 19 21 23 25 27 29
ω (GHz)

Figure 7

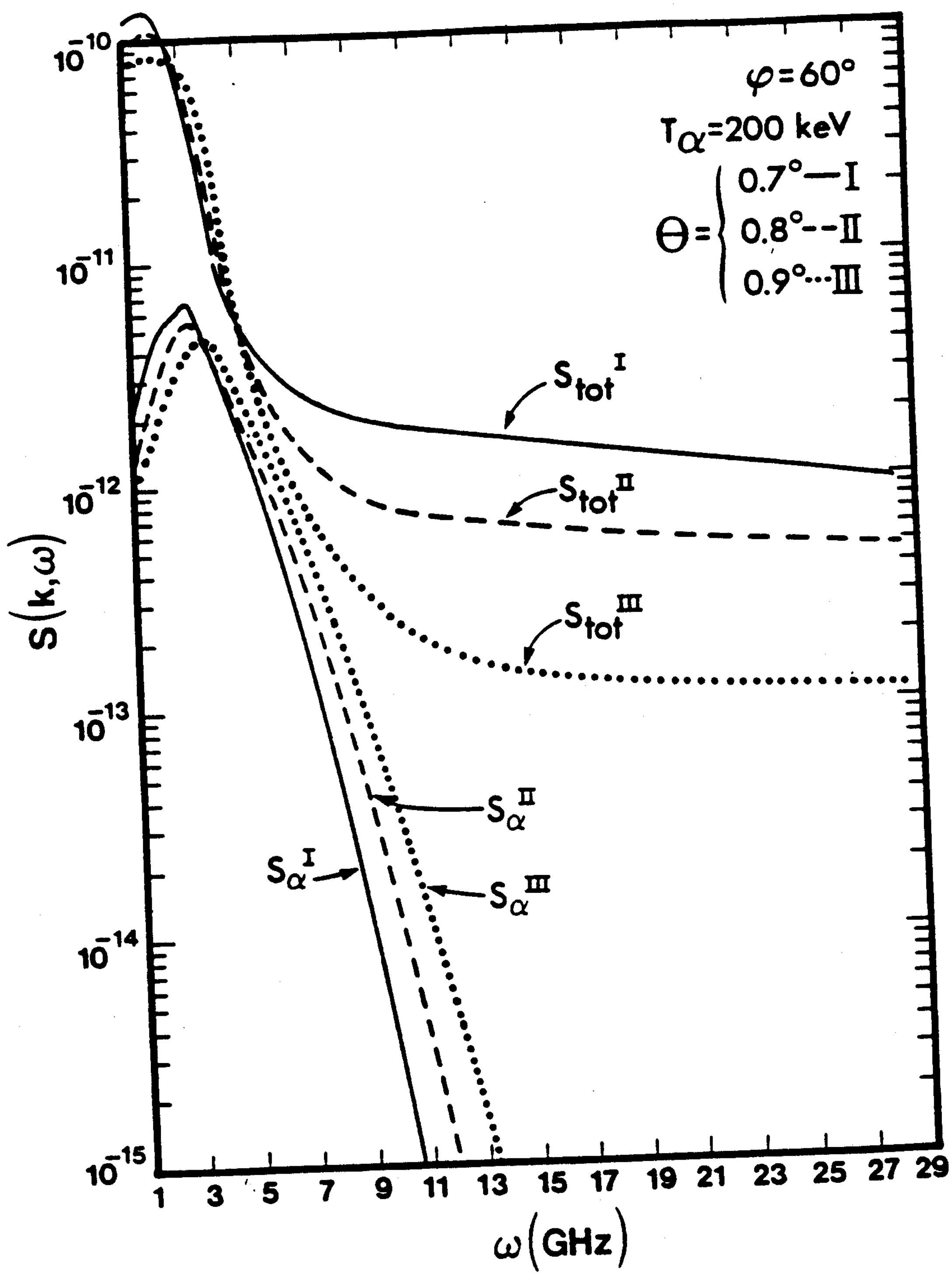

φ=60°
Tα=200 keV
Θ= 0.7°—I
0.8°--II
0.9°···III
S_tot^I
S_tot^II
S_tot^III
S_α^I
S_α^II
S_α^III
S(k,ω)
ω(GHz)
10^-10
10^-11
10^-12
10^-13
10^-14
10^-15
1 3 5 7 9 11 13 15 17 19 21 23 25 27 29

Figure 8

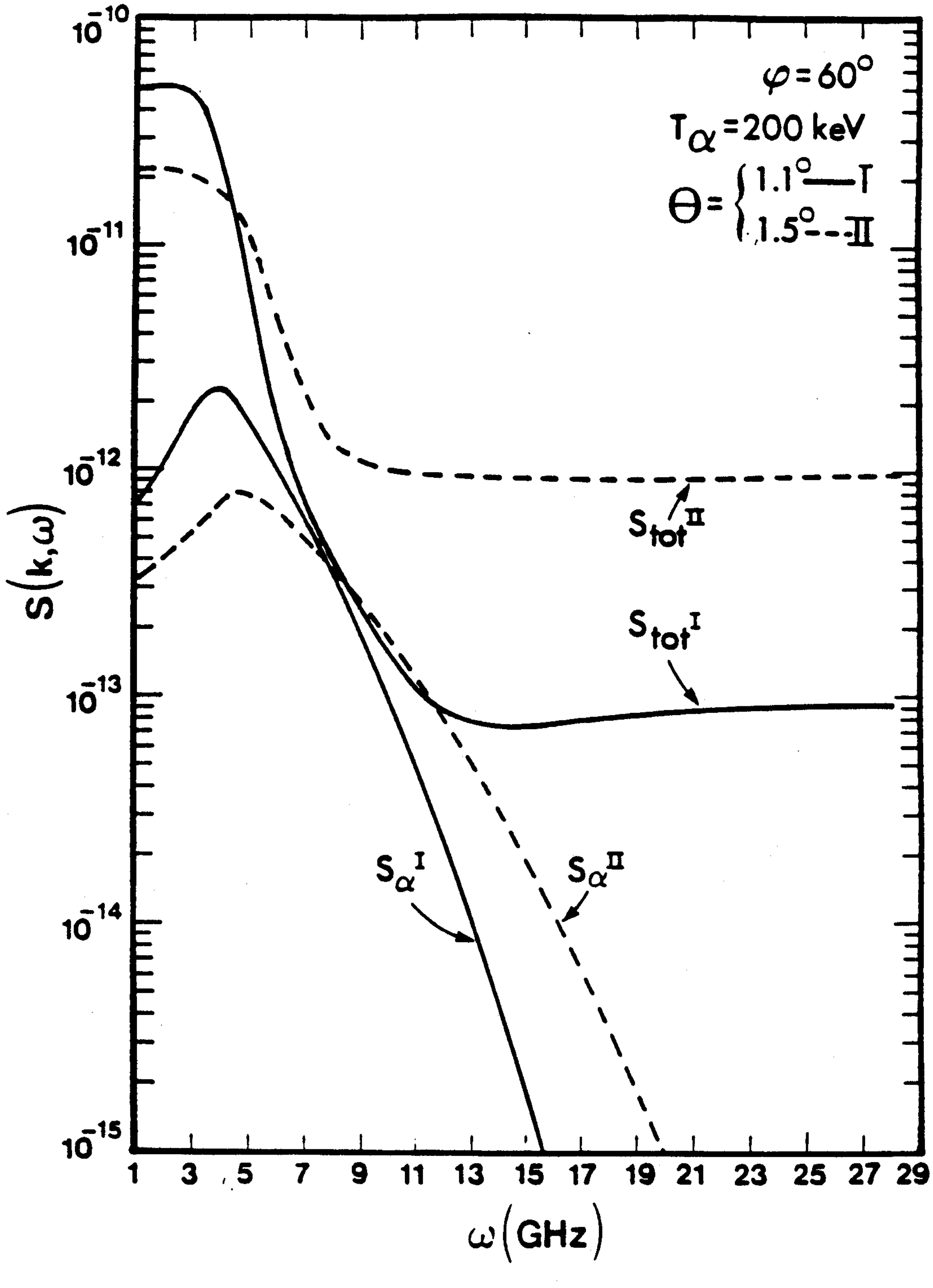

φ = 60°
Tα = 200 keV
Θ = { 1.1° —— I
1.5° - - - II
S(k,ω)
ω(GHz)
Stot II
Stot I
Sα I
Sα II
10^-10
10^-11
10^-12
10^-13
10^-14
10^-15
1 3 5 7 9 11 13 15 17 19 21 23 25 27 29

Figure 9

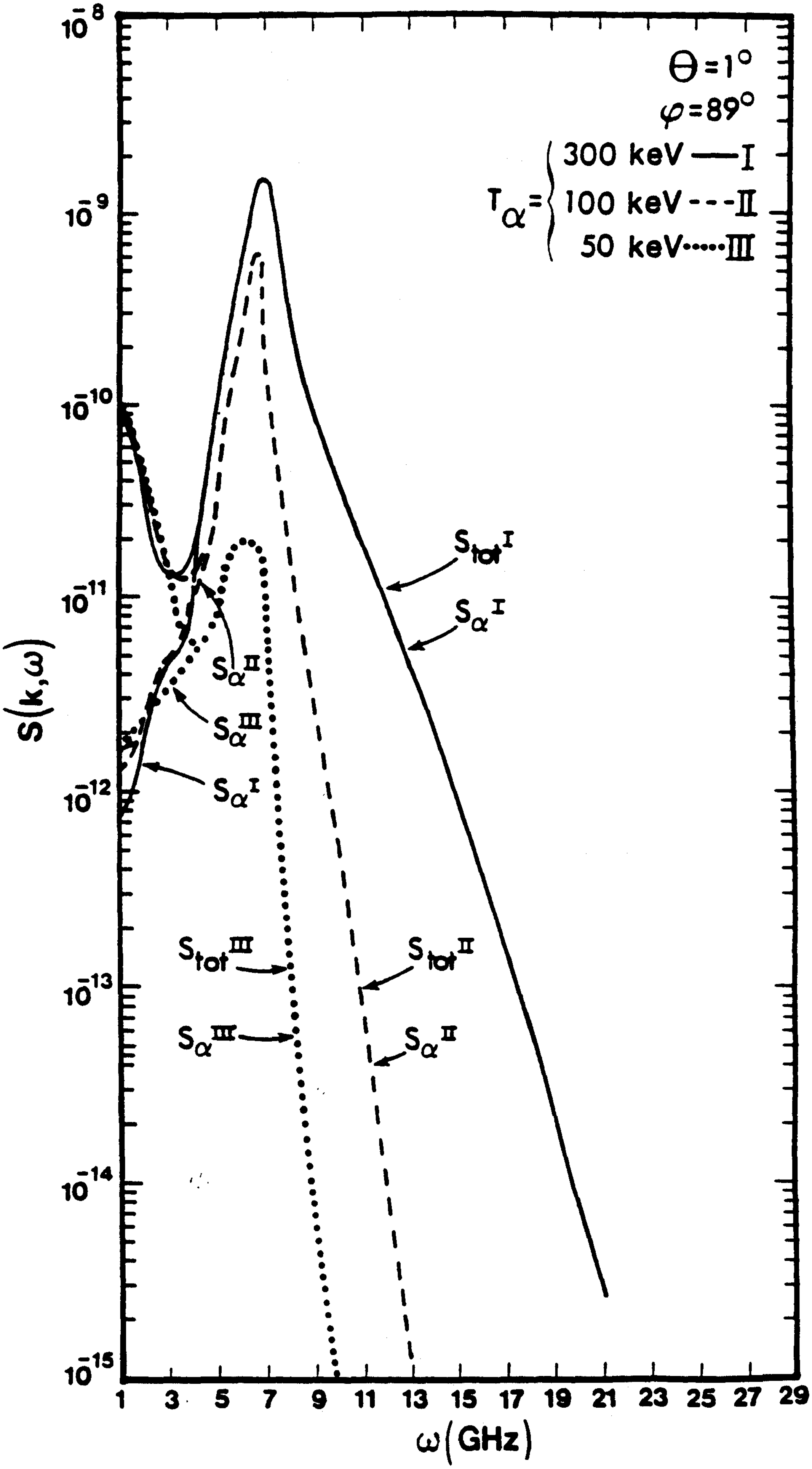

Θ=1°
φ=89°
T_α= 300 keV —— I
100 keV - - - II
50 keV ······ III
S_tot^I
S_α^I
S_α^II
S_α^III
S_α^I
S_tot^III
S_α^III
S_tot^II
S_α^II
S(k,ω)
ω(GHz)

Figure 10

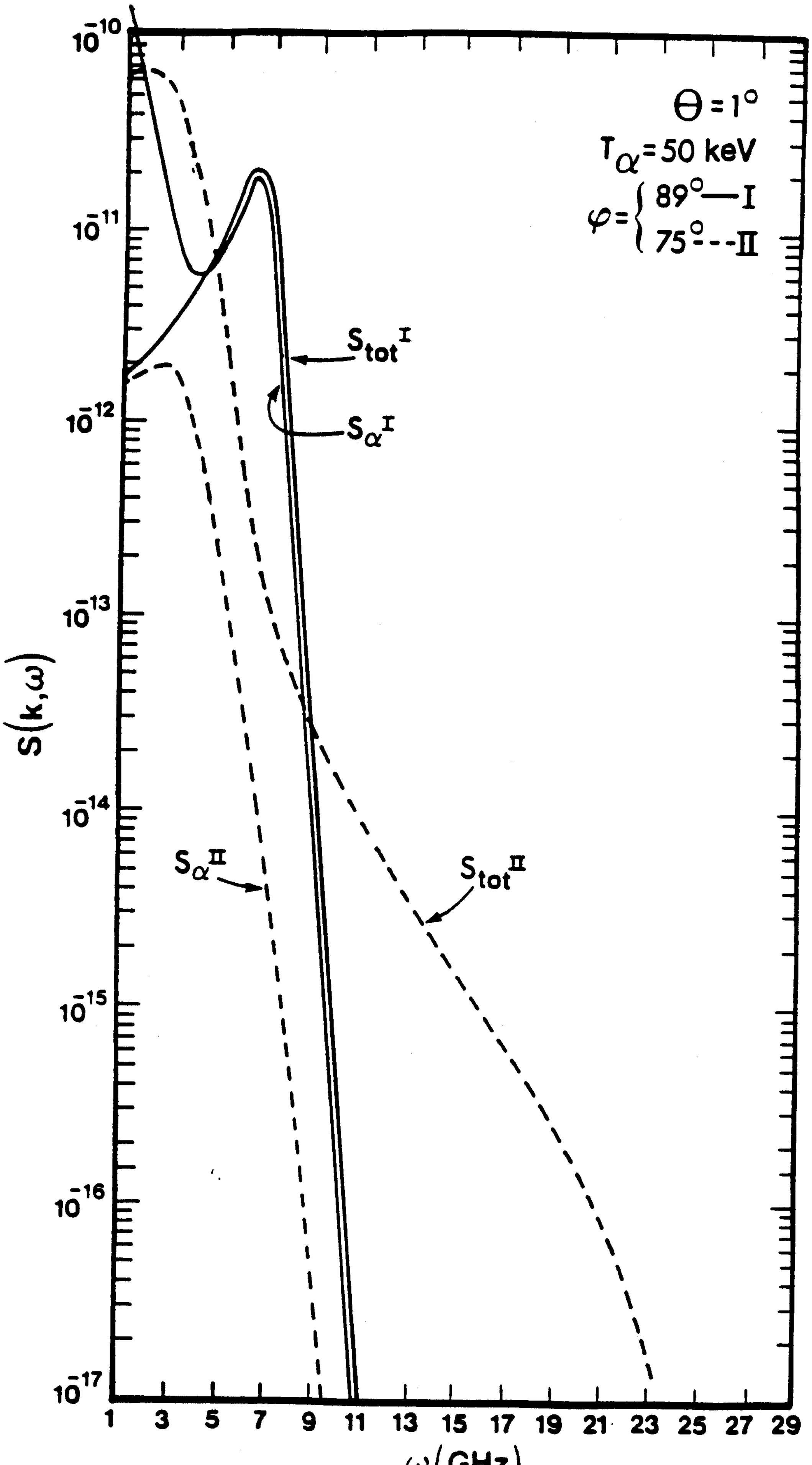

Θ = 1°
Tα = 50 keV
φ = { 89° — I
75° - - - II
S_tot^I
S_α^I
S_α^II
S_tot^II
S(k,ω)
10^-10
10^-11
10^-12
10^-13
10^-14
10^-15
10^-16
10^-17
1 3 5 7 9 11 13 15 17 19 21 23 25 27 29
ω(GHz)

Figure 11

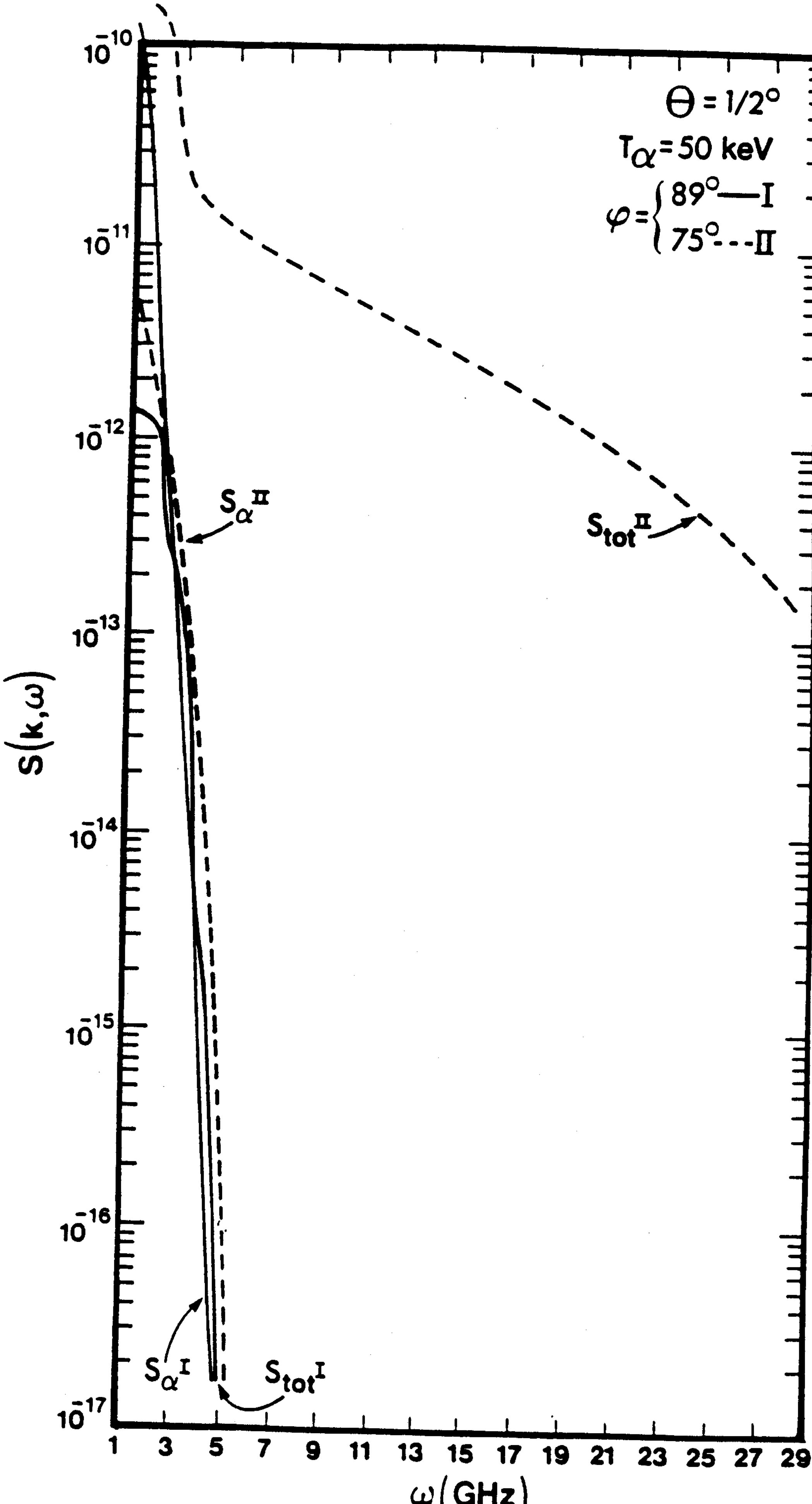

Θ = 1/2°
T_α = 50 keV
φ = { 89°—I, 75°---II
S_α^{II}
S_{tot}^{II}
S_α^{I}
S_{tot}^{I}
S(k,ω)
ω (GHz)
10^{-10}
10^{-11}
10^{-12}
10^{-13}
10^{-14}
10^{-15}
10^{-16}
10^{-17}
1 3 5 7 9 11 13 15 17 19 21 23 25 27 29

Figure 12

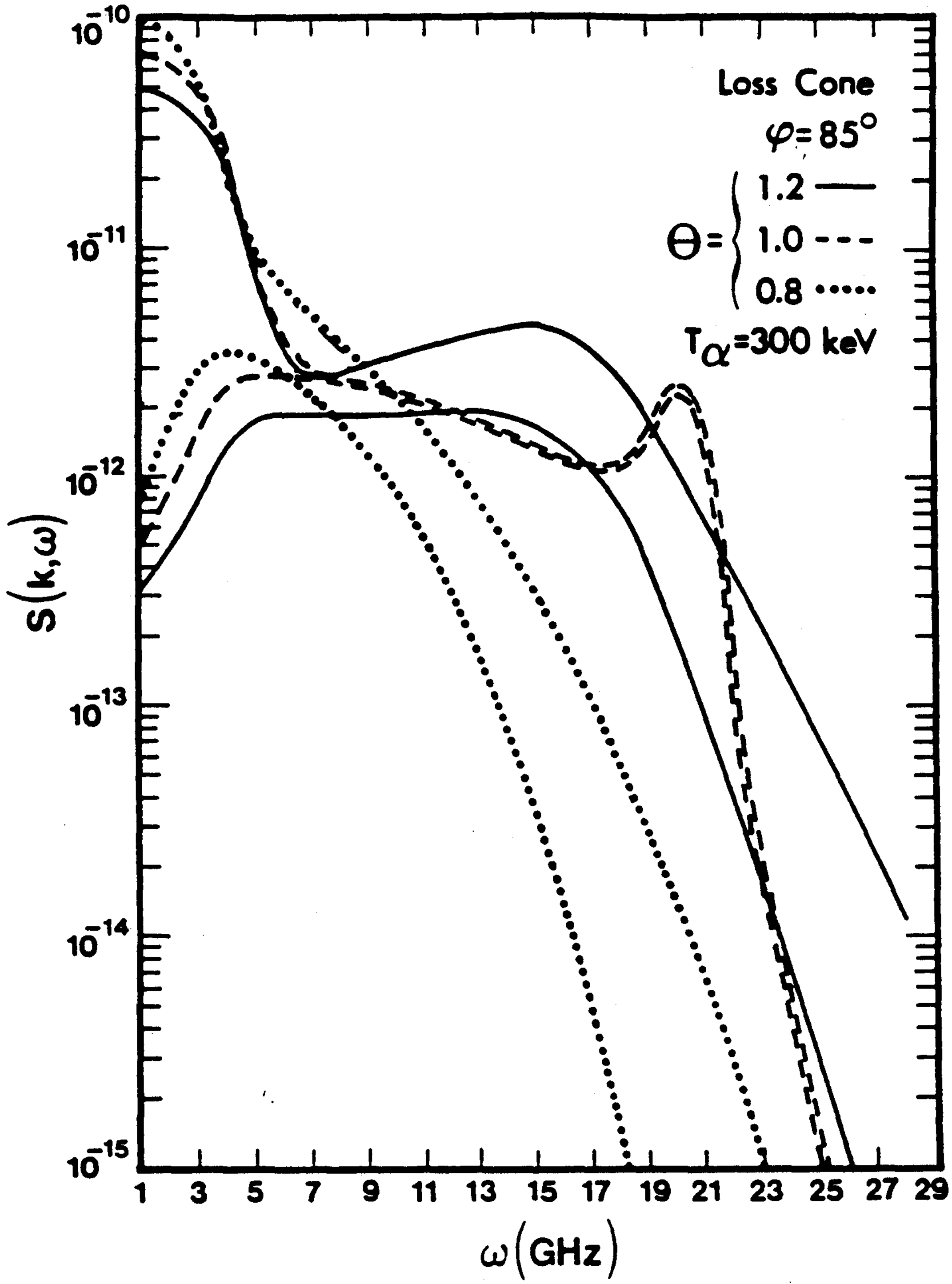

Loss Cone
φ=85°
Θ= 1.2
1.0
0.8
Tα=300 keV
S(k,ω)
ω(GHz)
10⁻¹⁰
10⁻¹¹
10⁻¹²
10⁻¹³
10⁻¹⁴
10⁻¹⁵
1 3 5 7 9 11 13 15 17 19 21 23 25 27 29

Figure 13